

Groundwater-controlled valley networks and the decline of surface runoff on early Mars

Keith P. Harrison and Robert E. Grimm

Southwest Research Institute, Boulder, Colorado, USA

Received 15 April 2005; revised 10 June 2005; accepted 28 July 2005; published 15 October 2005.

[1] Fluvial erosion on early Mars was dominated by valley networks created through a combination of groundwater processes and surface runoff. A reduced greenhouse effect due to CO₂ loss, together with a declining geothermal heat flux, promoted the growth of a cryosphere and a Hesperian hydrologic regime dominated by outflow channel formation. We test the hypothesis that the transition from valley network to outflow channel formation was preceded by a more subtle evolution characterized by a weakening of surface runoff, leaving groundwater processes as the dominant, final source of valley network erosion. Our hypothesis, supported by a terrestrial analog in the Atacama desert of Chile, is related to the groundwater sapping reactivation hypothesis for densely dissecting highland valley networks on Mars suggested by Baker and Partridge in 1986 and focuses on the age analysis of large, sparsely dissecting valley networks such as Nanedi Valles, Nirgal Vallis, valleys in fretted terrain, and tributaries of outflow channels and Valles Marineris chasmata. We find that these features are consistently late Noachian to Hesperian in age, younger than Noachian densely dissecting dendritic valley networks in the southern highlands. In the Tharsis region the observation of dense and sparse valley network morphologies on Hesperian terrain suggests that while surface runoff gave way to groundwater processes consistent with our hypothesis, the transition may have occurred later than elsewhere on the planet. The volcanic nature of Tharsis suggests that geothermal heat and volatile production led to episodically higher volumes of surface runoff in this region during the Hesperian.

Citation: Harrison, K. P., and R. E. Grimm (2005), Groundwater-controlled valley networks and the decline of surface runoff on early Mars, *J. Geophys. Res.*, *110*, E12S16, doi:10.1029/2005JE002455.

1. Introduction

[2] Fluvial features on Mars, being nearly as widespread in both age and location as impact craters, offer potentially valuable insight into regional and global aspects of Martian climate history, and surface and subsurface hydrology. The focus of this paper is on Noachian and Hesperian fluvial valleys, including the southern highlands dendritic networks and large individual valleys (e.g., Nanedi Valles, Nirgal Vallis, and valleys associated with fretted terrain). The formation of these features is generally attributed to some combination of surface runoff and groundwater sapping [e.g., Sharp and Malin, 1975; Laity and Malin, 1985; Pieri, 1976; Baker, 1982; Craddock and Howard, 2002] with secondary contributions from mass wasting and aeolian erosion and infilling [Carr, 1996].

[3] The initial discovery of dendritic valley networks in the southern highlands led some workers to infer an early “warm, wet” Martian climate capable of providing surface runoff through precipitation [Pieri, 1976; Pollack et al., 1987]. The need for a continuously wet Noachian climate remains to be satisfactorily established: episodic warm

periods may be sufficient [Christensen and Ruff, 2004]. Evidence for such periods is found in alluvial fans with valley meanders [Malin and Edgett, 2003; Moore et al., 2003], and crossbedding structures at Meridiani Planum thought to be formed by water currents [Squyres et al., 2004]. The erosive role of surface runoff is difficult to quantify, and at present can only be inferred by visual comparison of valley morphology with terrestrial counterparts. Such comparison suggests that a combination of dense drainage basin dissection, decreasing valley width downstream, “V”-shaped valley cross-section, and dissection of high-elevation watersheds, imply some surface runoff [Masursky, 1973; Carr, 1996; Craddock and Howard, 2002] (Figure 1a). In addition, most southern highlands valley networks also display some aspects of groundwater erosion (e.g., through sapping), and the assessment of fluvial erosive history is further complicated by a high degree of degradation through impact, aeolian and ice-related processes.

[4] Groundwater erosion processes may have dominated in large individual valleys, which are distinguished from the highlands dendritic networks by their theater-like headcuts, uniform width, and few, poorly developed tributaries [Laity and Malin, 1985; Kochel and Piper, 1986] (Figure 1b). In the descriptions that follow, these large valley networks are

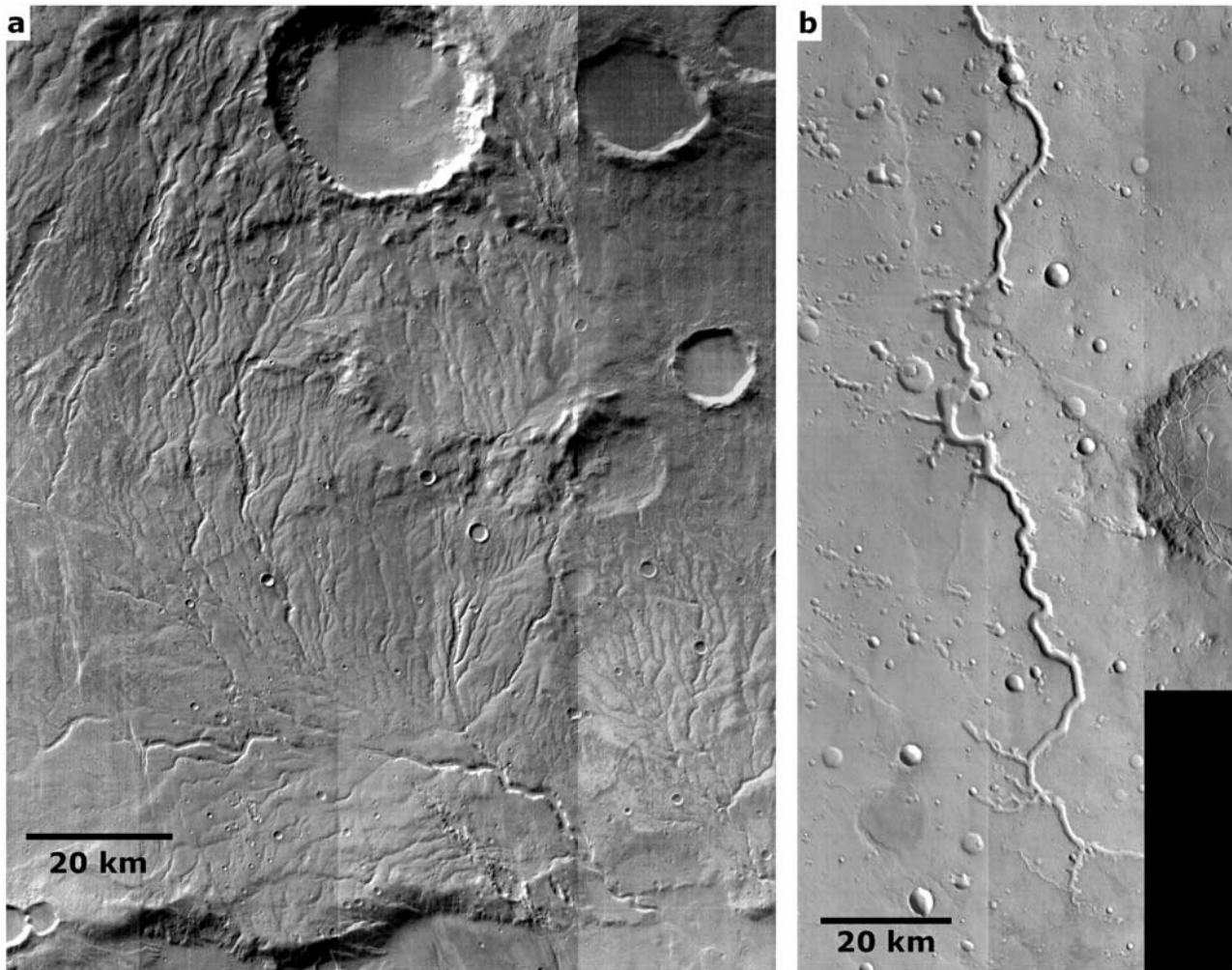


Figure 1. (a) THEMIS daytime mosaic of Warrego Valles on the southern boundary of the Noachian Thaumasia highlands. The drainage basin is densely dissected with many, well-developed tributaries, suggesting the influence of surface runoff. (b) THEMIS daytime mosaic of eastern Nanedi Vallis in Xanthe Terra. Tributaries and source regions are poorly developed and have theater-like headward morphologies, suggesting an origin through groundwater sapping. The tributaries shown here have a predominantly NW-SE trend, suggesting structural control. This does not necessarily constrain the mode of fluvial erosion, since runoff channels too may be influenced by structural heterogeneity. Note that image coordinates and identities for this, and other, figures are given in Table A1 in Appendix A.

called “sparse,” while dendritic, densely dissecting valley networks like those of the southern highlands are termed “dense.” The sparse networks, because of their size, relatively pristine condition, and clear morphological characteristics, appear to be more clearly associated with one class of formation processes, and it is on these networks that we focus in this work. The relationship with age suggested by the pristine condition of sparse valley networks plays a key role in the central hypothesis of this paper, which we describe in the following section.

2. Evolution of Fluvial Erosion

[5] In the late Noachian and early Hesperian a fundamental change in the Martian hydrologic cycle is indicated by the waning of surface runoff and groundwater sapping erosion, and the onset of catastrophic flooding events that carved the large outflow channels [Carr, 1996]. The initi-

ation of many of these channels in chaotic terrain suggests discharge of groundwater through disruptions in a confining cryosphere [Carr, 1979], a mode of fluvial activity not observed in dense and sparse valley networks.

[6] We suggest that the transition from valley network to outflow channel modes was preceded by a more subtle transition. In particular, we propose a shift toward groundwater-controlled valley network erosion (e.g., sapping) due to a decline in surface runoff. Before describing our hypothesis in greater detail, we review briefly the reason for its occurrence, namely climate change.

2.1. Early Martian Climate Change

[7] The predominantly Noachian age inferred for southern highlands dendritic valley networks [Scott and Dohm, 1992], together with high Noachian erosion rates inferred from crater degradation and mineralogic considerations [Chapman and Jones, 1977; Golombek et al., 2005], sug-

gest that a secular decline in atmospheric pressure early in Martian history occurred in order to produce the present climate [Jakosky and Phillips, 2001]. Atmospheric gases may have been ejected to space by impacts and interactions with the solar wind [Owen *et al.*, 1988; Melosh and Vickery, 1989; Luhmann *et al.*, 1992; Mitchell *et al.*, 2001], and may also have been sequestered in the polar caps and as crustal carbonates (although evidence for the latter is lacking [Bibring *et al.*, 2005]). The timing of loss to space was controlled by impact rates and by the longevity of the dipole magnetic field and its protective influence on the atmosphere. Impact rates were high in the early Noachian, continuing vigorously until a significant decrease between 3.8 and 3.5 Gyr ago [Hartmann and Neukum, 2001]. Analysis of the Allan Hills 84001 meteorite suggests that significant atmospheric loss had already occurred 4 Gyr ago [Sugiura and Hoshino, 2000], although a likely late heavy bombardment between 3.9 and 3.8 Gyr ago [Hartmann *et al.*, 2000] implies a similarly timed spike in atmospheric loss. The timing of dipole field cessation is less certain and is constrained only by crustal magnetic anomaly age estimates, which range from 4.2 Gyr ago to something less than 4.0 Gyr ago [Stevenson, 2001, and references therein].

[8] The behavior of the Martian climate was undoubtedly influenced by atmospheric sources as well as sinks. These include regional volcanic centers such as the Tharsis rise, which was largely complete by the end of the Noachian [Phillips *et al.*, 2001], and impact sources. The potentially large yet sporadic nature of these contributions, coupled with widely ranging planetary obliquity and eccentricity, raises the possibility of a highly dynamic early atmosphere permitting perhaps only episodic fluvial erosion [e.g., Dohm *et al.*, 2000].

[9] Temperatures attending climate change are uncertain. The formation of Noachian valley networks may have required temperatures above freezing and therefore a significant greenhouse [Pollack *et al.*, 1987]. However, the several bars of CO₂ required for such a greenhouse [Kasting, 1991; Mischna *et al.*, 2000] are difficult to simulate in climate models [e.g., Haberle, 1998] and were, perhaps, present only during major outgassings from Tharsis and other volcanic regions [Dohm *et al.*, 2000]. An alternative view has the Noachian valley networks forming in subfreezing temperatures, with water supplied by melting at the base of ice sheets [Carr and Head, 2003]. Where no basal melting occurs, a cryosphere develops but, like the ice sheets, is limited in thickness by the relatively high Noachian geothermal heat flux [Schubert *et al.*, 1992].

2.2. Hypothesized Evolution of Fluvial Erosion

[10] Greenhouse weakening associated with CO₂ loss during early Martian climate change greatly reduced the quantity of water vapor in the atmosphere through the processes described above (sequesterization in crust and polar caps [Jakosky and Phillips, 2001] and loss to space through impacts and interaction with the solar wind [Jakosky and Leshin, 2001]). We propose that the depletion of atmospheric water vapor had a fundamental impact on fluvial erosive style that was, at least to some degree, independent of the early temperature regime and of the temporal fluctuations in fluvial activity (i.e., episodic or continuous). Our hypothesis follows from the standard

model of infiltration [e.g., Fetter, 1994] in which surface runoff occurs only when the infiltration capacity of the subsurface has been exceeded. We suggest that this state of excess occurred (at least episodically) during the Noachian, with fluvial features from this epoch bearing the mark of at least some surface runoff erosion. Water may have been supplied by rainfall or by basal melting of ice sheets. In the late Noachian and early Hesperian, when available volumes of atmospheric water vapor declined, the majority of the (now reduced) liquid surface water supply was able to infiltrate the crust, leading to fluvial erosion more clearly dominated by groundwater processes.

[11] In the case of a warmer early atmosphere, a simple decrease in precipitation rate (perhaps accompanied by more limited spatial coverage) would have led to this change. In the case of a colder early atmosphere, basal melting, which occurs at a rate controlled in part by surface accumulation [Clifford and Parker, 2001], would also have slowed and become more spatially limited. The cold scenario would also have been affected by the continually decreasing geothermal heat flux [Schubert *et al.*, 1992], which would have reduced the surface water supply by increasing the critical ice sheet thickness required for basal melting. Note that the warm and cold scenarios both end with a thick Hesperian cryosphere. On a warm early Mars, the cryosphere would start forming when climate change forced surface temperatures below freezing. On a cold early Mars, a thin cryosphere would already be in place and would simply expand to Hesperian dimensions in response to temperature changes (if any) and decreasing geothermal heat flux. In reality, climate change likely involved some combination of the warm and cold scenarios. Whatever this combination, the overall decrease in atmospheric volatile content would, we suggest, have resulted in a net decrease in the surface water supply and a greater emphasis on groundwater-controlled fluvial erosion.

[12] We note that infiltration likely continued to be an important source of aquifer recharge throughout the hypothesized evolution, an idea supported by high elevation sapping features with access to aquifers too small to store instantaneously the volumes of water thought to have produced the observed fluvial erosion [Craddock and Howard, 2002].

[13] We note further that reduced spatial coverage of surface water delivery during climate change may have favored certain locations. In particular, precipitation may have retreated to those regions predicted by climate models to experience enhanced rain or snowfall. These locations generally depend on the planetary obliquity (which is thought to have varied widely over Martian history [Laskar *et al.*, 2004]) and include the polar regions (at low obliquities) and low-latitude regions (at high obliquities), especially those with elevated topography and thermal inertia [Mischna *et al.*, 2003]. Tharsis is therefore a likely location for enhanced precipitation at high obliquities. Significant volcanic outgassing and enhanced geothermal heat may also have intensified regional precipitation and infiltration, respectively. Again, Tharsis is a suitable candidate, and is discussed further in this capacity below. Finally, impacts themselves may have influenced regional climate [Segura *et al.*, 2002], but we do not consider this phenomenon further.

[14] Our fluvial evolution hypothesis has elements in common with that of *Baker and Partridge* [1986], who identified (in Viking images) Martian groundwater sapping and surface runoff morphologies within individual southern highlands dense valley networks. The preferential downstream location of sapping valleys suggested to *Baker and Partridge* [1986] that a younger epoch of groundwater-controlled fluvial erosion followed initial incisement influenced by surface runoff. Only a small number of subsequent analyses using more recent data have revisited this idea, with some providing support [e.g., *Williams and Phillips*, 2001] and some not [e.g., *Cabrol and Grin*, 2001]. Other analyses of Martian fluvial erosion history suggest distinct epochs of activity [*Neukum and Hiller*, 1981; *Grant and Schultz*, 1993; *Hynek and Phillips*, 2001; *Irwin et al.*, 2005] but not an accompanying change in erosive style.

[15] The scope of our hypothesis, unlike that of *Baker and Partridge* [1986], attempts to include the large sparse valley networks of Mars, shifting the focus from small, degraded examples of sapping morphology to more pristine features including those with clearer relationships to other morphologies. The remainder of this paper serves to test our hypothesis by arguing that dense and sparse networks formed on Mars at times commensurate with the proposed evolution, namely that dense valley networks (excluding those with obvious local water sources, such as valleys on volcano flanks) are predominantly Noachian, and sparse networks are predominantly late Noachian and early Hesperian. We present first a broad global age analysis, followed by discussions of individual networks and, finally, a description of a terrestrial analog, along with other concluding remarks.

3. Global Overview

3.1. Age Analysis

[16] The simplest way to constrain the age of a valley network is to measure the age of the geologic unit(s) it incises. This approach provides an upper bound on age only: the most recent fluvial erosion in a valley cannot be older than the youngest unit the valley incises. Dating actual valley floors is difficult because the sampling surface is small and crater numbers tend to be low. Also, including small craters may raise secondary cratering issues [e.g., *McEwen*, 2003]. Nonetheless, such analyses may still be useful and, where available, are reported below.

[17] Before considering specific examples of valley network age analyses, we present a broad global indication of dense and sparse valley network ages based on their underlying geological units. We superimposed Martian valley networks [*Carr and Clow*, 1981] onto geologic units [*Greeley et al.*, 1987] grouped into six epochs (early, middle, and late Noachian, early and late Hesperian, and Amazonian [after *Tanaka*, 1986]). The age of each contiguous set of valley network pixels was approximated by the epoch of the geologic units it crossed. If it crossed units belonging to more than one epoch, its age was determined by that epoch representing the greatest fraction of the total valley network length. An alternative, and perhaps theoretically superior, approach is to choose the youngest of the epochs underlying the valley network, but this method is

Table 1. Location and Approximate Age of Sparse Martian Valley Networks^a

Valley Network	Lat.	Lon.	Age ^b	Distance to Tharsis, ^c km
Huo Hsing Vallis	32°N	66°E	MN	9654
Auqakuh Vallis	29°N	61°E	MN	9430
Scamander Vallis	16°N	29°E	MN	8083
Unnamed Valley	10°S	142°E	MN	6641
Unnamed Valley	12°S	144°E	MN	6445
Al Qahira Vallis	18°S	163°E	MN	5392
Ma'adim Vallis	12°S	177°E	MN	4373
Sabrina Vallis	11°N	311°E	LN	3347
Nanedi Valles	6°N	311°E	LN	3263
Licus Vallis	3°S	126°E	EH	7528
Mamers Valles	42°N	16°E	EH	7368
Mad Vallis	58°S	77°E	EH	6329
Nirgal Vallis	28°S	318°E	EH	3761
Bahram Vallis	21°N	301°E	EH	3217
Louros Valles	9°S	278°E	EH	1442
Echus Chasma Canyons	0°N	278°E	EH	1430
Unnamed Valley	25°N	237°E	LH	2456
Rhabon Valles	22°N	270°E	A	2036

^aThe Ismeniae Fossae valley near Mamers Valles is not in the valley network database used for this analysis and so does not appear in the table.

^bAges are derived from the data in Figure 2. MN, middle Noachian; LN, late Noachian; EH, early Hesperian; LH, late Hesperian; A, Amazonian.

^cDistances are measured along the great circle connecting the valley network to the center of Syria Planum.

more susceptible to errors in the coregistration of valley network and geologic maps at the spatial resolution used here (quarter degree). The final step of the procedure was to use Mars Odyssey THEMIS infrared and visual images and, when necessary, Mars Global Surveyor MOC and MOLA data, to designate each valley network as either dense or sparse. We were conservative in assigning networks to the latter category (Table 1): a total of 18 sparse networks were accumulated (compared to several hundred dense valley networks).

[18] The results of the analysis are presented using a “network density” parameter, defined as the number of valley networks from a particular epoch divided by the total surface area of geologic units belonging to that epoch. (Note that this density is not the same as drainage density, which measures the total valley length per unit area within a single valley network.) Because there are many times more dense networks than sparse networks, network densities for dense networks tend to be higher than for sparse networks and we normalize the data for each morphology to its average network density. A histogram of the data (Figure 2a) suggests that dense valley network formation was most prevalent in the early and middle Noachian, began declining in the late Noachian, and occurred only occasionally in the Hesperian and Amazonian. Sparse valley network formation, on the other hand, appears to have peaked in the late Noachian and continued at modest levels throughout the Hesperian. We note that the late Noachian age bin for sparse valley networks represents only two of the 18 sparse networks (Nanedi and Sabrina Valles), whereas the early Hesperian age bin contains six. The emergence of the groundwater fluvial regime may thus be more accurately assigned an early Hesperian age. We note that Figure 2 shows no sparse valley networks in the early Noachian. This is due principally to our conservative categorization criteria for sparse valley networks, which result in relatively low

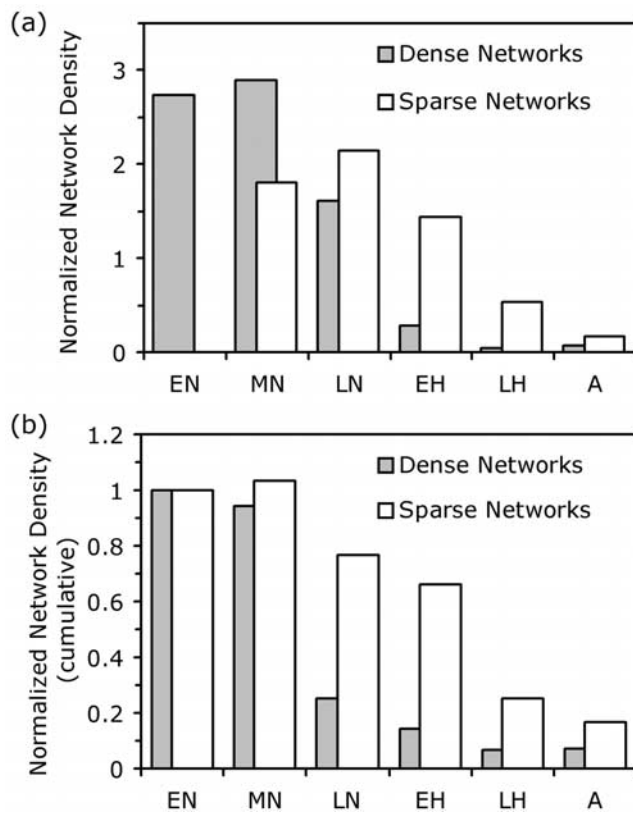


Figure 2. (a) Normalized network densities (defined in text) demonstrate an early to late Noachian period of dense valley network formation, and a predominantly late Noachian period of sparse valley network formation, with activity continuing throughout the Hesperian. (EN, early Noachian; MN, middle Noachian; LN, late Noachian; EH, early Hesperian; LH, late Hesperian; A, Amazonian). (b) A more conservative approach groups all valleys of a particular age and younger; the resulting normalized network densities are shown. Values for the late Noachian and younger epochs again indicate relatively greater sparse network activity.

counts in all age bins, and therefore a reasonable probability of a zero count. Some characteristics of sparse network morphology are indeed observed on early Noachian terrain, but their relationship to contiguous dense valley segments is unclear, and they do not qualify here as “sparse.”

[19] A more conservative approach recognizes that no lower bound on ages can be imposed using underlying geological unit ages. Network densities are thus calculated by dividing the number of sparse or dense networks of a particular age and younger by the total surface area corresponding to the same age range. The densities are then normalized by the same average values used in the previous approach. The results (Figure 2b) again indicate a relatively enhanced frequency of sparse networks from the late Noachian to the Hesperian, and a corresponding decline in dense network formation.

3.2. Statistical Tests

[20] A χ^2 statistical analysis of the valley network frequencies contributing to Figure 2a suggests that sparse

and dense valley networks do, indeed, have distinct relationships with age (at a confidence level better than 0.001). These relationships support our central hypothesis, and are consistent with other general age assignments [e.g., Tanaka, 1986]. We also compared a further three properties of the sparse and dense valley network populations, namely elevation, latitude, and proximity to Tharsis. While mean elevations and latitudes were somewhat lower for sparse networks, standard deviations were large enough to eschew significance in these differences. Proximity to Tharsis also did not produce a statistically significant difference between the sparse and dense populations. However, the distribution of networks within the sparse population alone does appear to relate to Tharsis (Table 1). Specifically, the middle Noachian sparse network bin of Figure 2 contains networks located relatively far from Tharsis on the crustal dichotomy boundary between about 60°E and 180°E and in the southern highlands, while the late Noachian bin contains valleys closer to Tharsis (Nanedi and Sabrina Valles). Four of the seven early Hesperian networks are close to Tharsis, while two are close to other volcanic centers (Elysium Mons and Amphitrites Patera). In the concluding discussion we suggest a mechanism which may have produced the trend in proximity to Tharsis. We note that a similar relationship within the dense valley network population was not observed.

[21] The relatively small number of sparse networks, and their distribution on a wide range of terrains, warrant a more detailed study of age relationships, and to this end we devote the next section of the paper. The southern highland valley networks, which constitute the majority of dense valley networks, have long been assigned a largely Noachian age [Scott and Dohm, 1992; Carr and Chuang, 1997]. We accept this assertion and focus on the large groundwater sapping networks of Mars, starting with individual analyses of features in Xanthe Terra, Lunae Planum, Margaritifer Sinus, and in fretted terrains. We then discuss sapping morphologies associated spatially with outflow channels and with dense valley networks.

4. Regional Analyses

4.1. Xanthe Terra

[22] Xanthe Terra is a region of ancient, heavily cratered terrain south of the Chryse basin, bounded to the east by the circum-Chryse outflow channels, and to the west by the Hesperian ridged plains of Lunae Planum. Most of Xanthe Terra is covered by the late Noachian subdued crater unit (Np1₂) [Rotto and Tanaka, 1995] which encompasses Nanedi Valles, the largest valley network in the region. Nanedi Valles exhibits typical groundwater sapping morphology, with few, poorly developed tributaries, uniform valley width, and theater-like head regions (Figure 1). It is also relatively pristine, with steep walls delineated sharply from the surrounding terrain. Fluvial activity was likely episodic, as suggested by a narrow inner valley [Carr and Malin, 2000], an alluvial fan, and an abandoned valley segment (Figure 3a).

[23] Rotto and Tanaka [1995] designate the valley floor as unit HNcv (late Noachian to early Hesperian smooth valley floor). We found superimposed on Nanedi Valles 16 craters greater than 1 km in diameter, yielding an

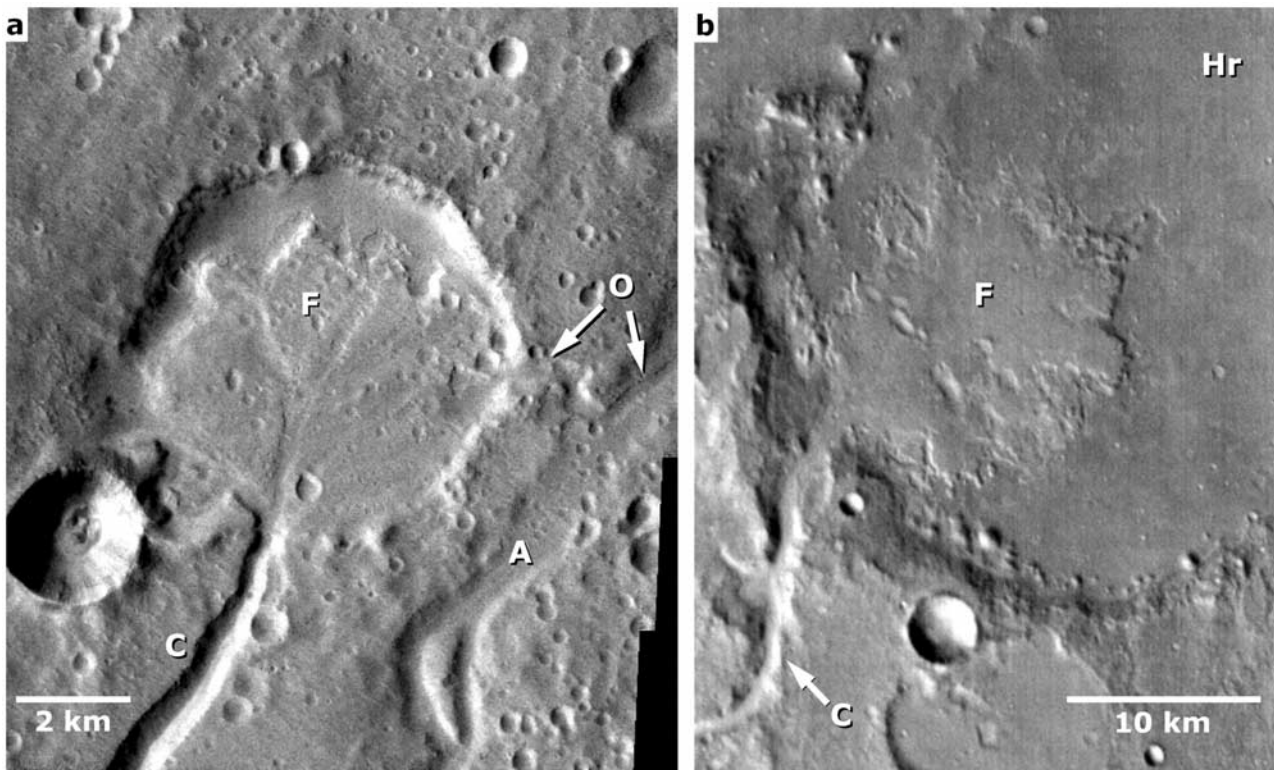


Figure 3. (a) The main valley of north Nanedi Vallis (C) enters a crater and splits into smaller valleys over an alluvial fan (F). A break in the east crater wall allows an outlet valley (O) to be carved in the main valley (A) which was abandoned in favor of valley C. THEMIS visual image. (b) North of Nanedi Vallis, Sabrina Vallis (C) ends its course at an alluvial fan (F) which appears to overlie Hesperian ridged plains material (Hr). MOC imagery, however, suggests a more complex relationship. THEMIS IR daytime.

$N(1)$ value of 3880 ± 970 such craters per 10^6 km^2 . This range of values spans very closely the *Tanaka* [1986] definition of the early Hesperian epoch ($3000 < N(1) < 4800$) and falls within the *Rotto and Tanaka* [1995] age interval.

[24] Other valleys in Xanthe Terra designated as HNCv [Rotto and Tanaka, 1995] include Sabrina and Drilon Valles. Sabrina Vallis empties onto an alluvial fan which appears to overlie a ridged plains unit (Figure 3). THEMIS and MOC images reveal this unit to be part of a larger Hr deposit to the north, suggesting (at the oldest) an early Hesperian age for the Sabrina Vallis fan. However, the precise relationship between fan and surrounding volcanic flows is not without uncertainty, and the presence of possible outlying fan segments embayed by the Hr unit, and indications of collapse within the fan due to volatile release, may indicate the reverse age relationship.

4.2. Lunae Planum

[25] Lunae Planum lies to the west of Xanthe Terra, with Kasei Valles bounding it to the west. The largest valley network in Lunae Planum is Bahram Vallis (Figure 4). This pristine valley, which is morphologically similar to Nanedi, Sabrina, and Drilon Valles, must be at most early Hesperian in age since much of its length incises the Hesperian ridged plains material of Lunae Planum. In addition, crater counting on the Bahram Vallis floor yields ages of early to late Hesperian [Neukum and Hiller, 1981].

4.3. Margaritifer Sinus

[26] The Margaritifer Sinus region, north of the Argyre impact basin, is a complex superposition of different fluvial morphologies. The largest feature is a wide depression running northward from the Argyre basin to Margaritifer and Iani Chaotes. The depression narrows in places to form Uzboi and Ladon Valles. Entering this system from the east is a series of densely dissecting drainage networks including Parana-Loire and Samara Valles. The only large network entering the Uzboi-Ladon system from the west is Nirgal Valles (Figure 5), a typical example of groundwater sapping morphology [Jaumann and Reiss, 2002], and relatively pristine. Nirgal incises middle and late Noachian units (Np_1 and Np_2) [Greeley et al., 1987] and contains Hesperian “older valley material” (unit Hch). Grant and Parker [2002] suggest an early Hesperian cessation to groundwater sapping in the region. Specifically, they infer that late stage flow in Nirgal Vallis contributed to the final (i.e., Hesperian) stages of fluvial activity in Margaritifer Sinus.

4.4. Fretted Valleys

[27] Fretted terrain occurs along the crustal dichotomy boundary in two broad zones, one between 0°E and 80°E (north Arabia Terra), and the other between 120°E and 180°E (north Cimmeria Terra). The morphology in both zones is characterized to first order by cratered highland remnants in the form of mesas separated by lowlands material. The mesas become smaller further northward

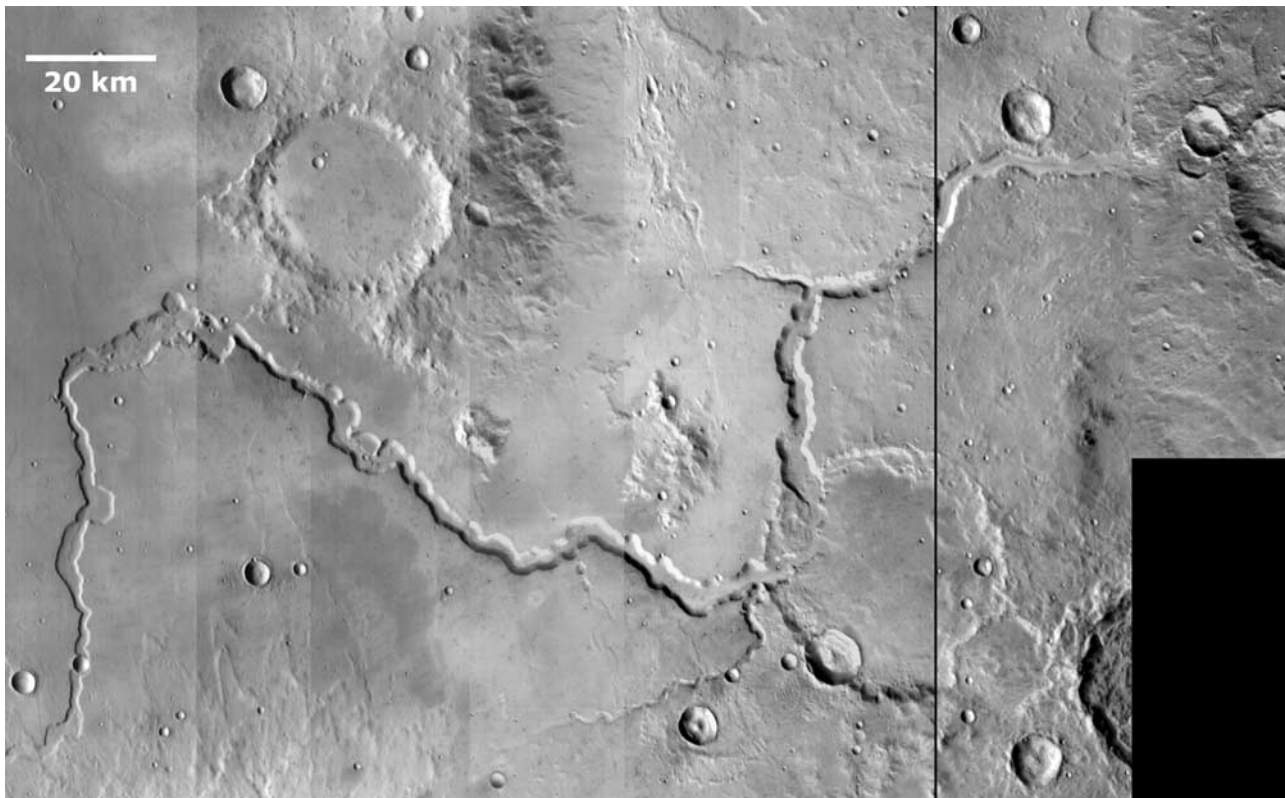


Figure 4. THEMIS IR daytime mosaic of Bahram Vallis. The downstream direction is from left to right. The upstream half of the valley crosses Hesperian ridged plains (Hr), while the downstream half incises Noachian dissected terrain (Npld). A groundwater sapping origin is inferred from the small number of tributaries, the roughly uniform valley width, and theater-like headward termini.

and grade into knobby terrain [Sharp, 1973; Parker *et al.*, 1989]. Mass wasting and ice-related processes in the north Arabia Terra fretted terrain (which lies between 30°N to 50°N) are thought to have widened valleys and produced features such as debris aprons and lineated valley fill [Carr, 2001] not observed in the more volatile-poor lower latitudes of the Cimmeria Terra terrain.

[28] Only a small number of fluvial valleys are observed in (and adjacent to) the Arabia Terra fretted terrain, and include Mamers Vallis and the Ismeniae Fossae valley. They have theater-like tributary headcuts and few tributaries, suggesting a sapping origin (Figure 6) [Sharp and Malin, 1975]. McGill [2000] notes that the presence of closed depressions in the Ismeniae valley source region

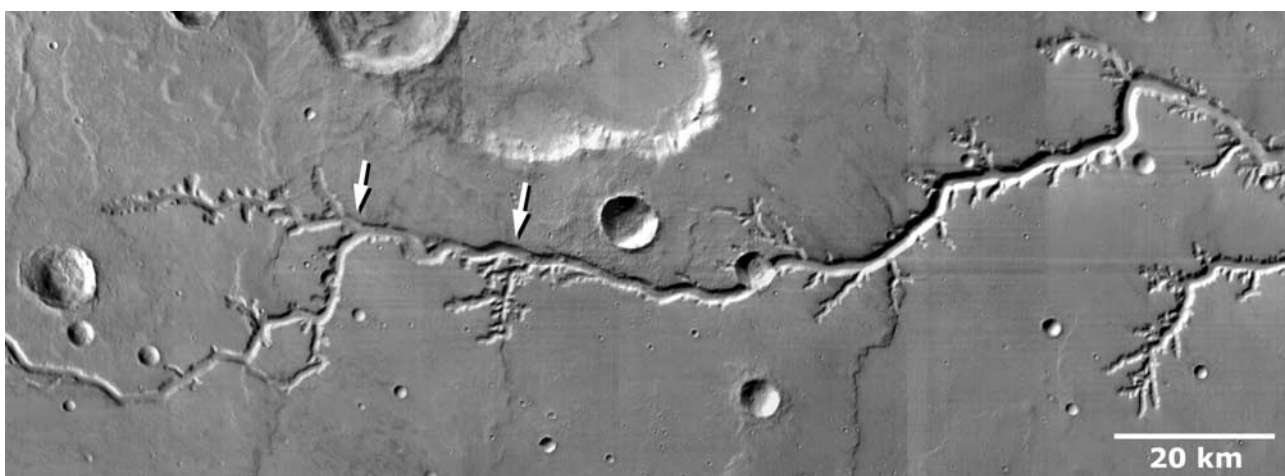


Figure 5. THEMIS IR daytime mosaic of Nirgal Vallis. Typical sapping characteristics include uniform valley width and theater-like source regions. Some structural control is observed (arrows).

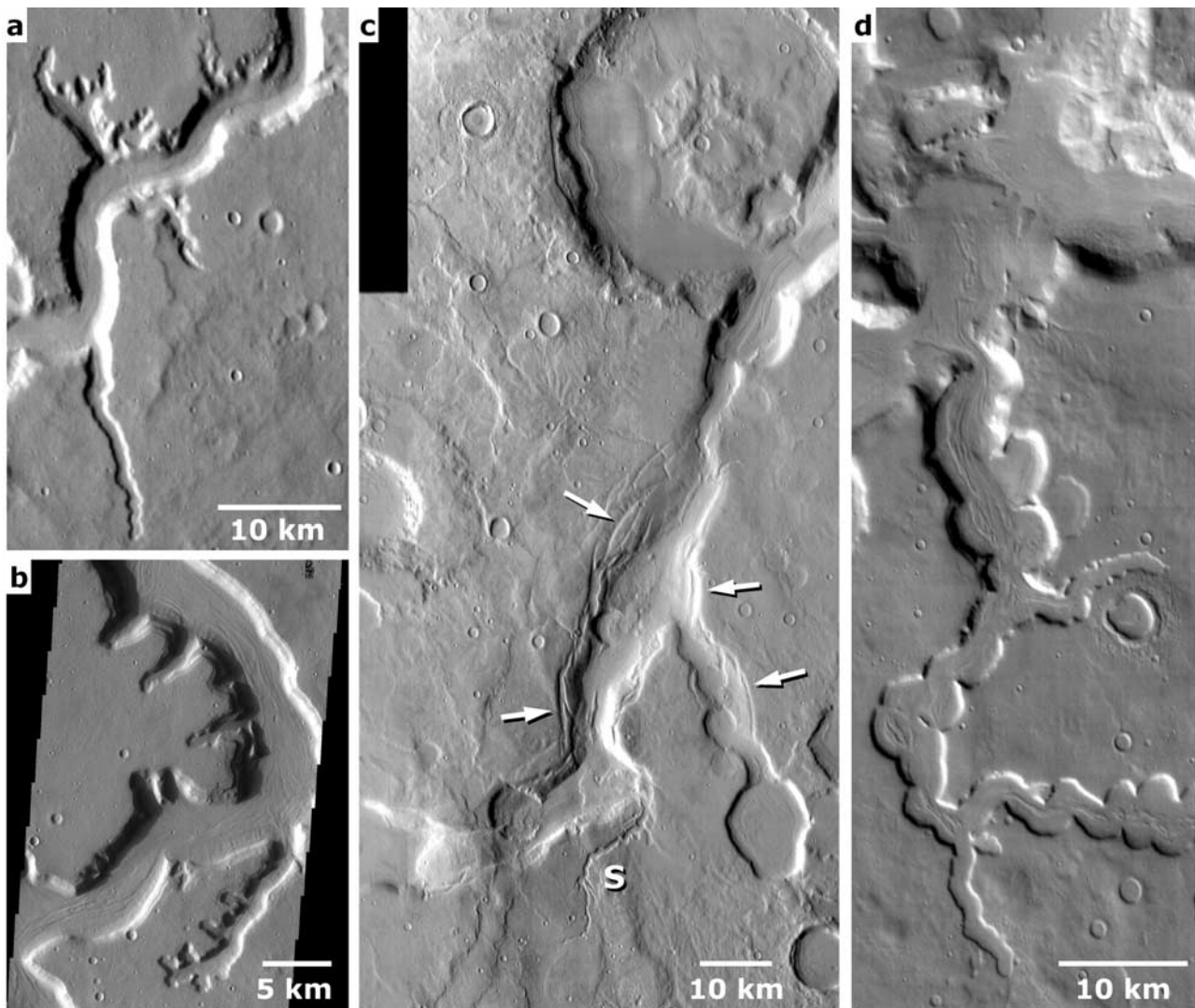


Figure 6. (a) THEMIS IR daytime and (b) THEMIS visual images of sapping tributaries along Mamers Vallis. (c) Elongate depressions in the source region of the Ismeniae channel are bounded by fractures (arrows) suggesting collapse following removal of subsurface material. The west depression lies on the flanks of a possible volcanic structure (off left image edge). Note the sapping tributary (S). THEMIS IR daytime mosaic. (d) Sapping morphology in the Ismeniae valley. THEMIS IR daytime.

may indicate erosion by surface runoff fed by lakes. However, some of the depressions appear to have formed through collapse due to subsurface removal of material (Figure 6) and therefore support a groundwater-controlled origin. The source of groundwater may be related to nearby volcanism [Carruthers and McGill, 1998] in which case the valley may have formed through catastrophic discharge of water melted by volcanic heat, an origin more closely associated with outflow channel processes (although typical outflow morphologies such as chaotic terrain and streamlined islands, that would be difficult to obscure with subsequent mass wasting, are not observed). If the Ismeniae feature is an outflow channel, an analysis of its age remains useful for a later discussion of its tributaries. Crater counting data [McGill, 2000] suggest an early Hesperian age, in agreement with an estimated late Noachian to early Hesperian period of formation for all fluvial valleys in the region [Tanaka, 1986; Carr,

2001]. Mamers Vallis incises heavily eroded Noachian terrain but also passes through Hesperian ridged plains (unit Hr) [Greeley *et al.*, 1987], further suggesting an early Hesperian age. Mamers Vallis and the Ismeniae valley are well preserved, consistent with a post-heavy bombardment formation time. However, more recent back wasting of valley walls may have altered the fluvial morphology, leading to a continued pristine appearance and the downstream increase in valley width unique to this region [Carr, 2001].

4.5. Sapping Morphology Associated With Outflow Channels and the Valles Marineris

[29] Support for a late Noachian to Hesperian dominance of groundwater sapping processes over surface runoff is observed in sapping morphologies related to larger features of that age such as the circum-Chryse outflow channels and the Valles Marineris.

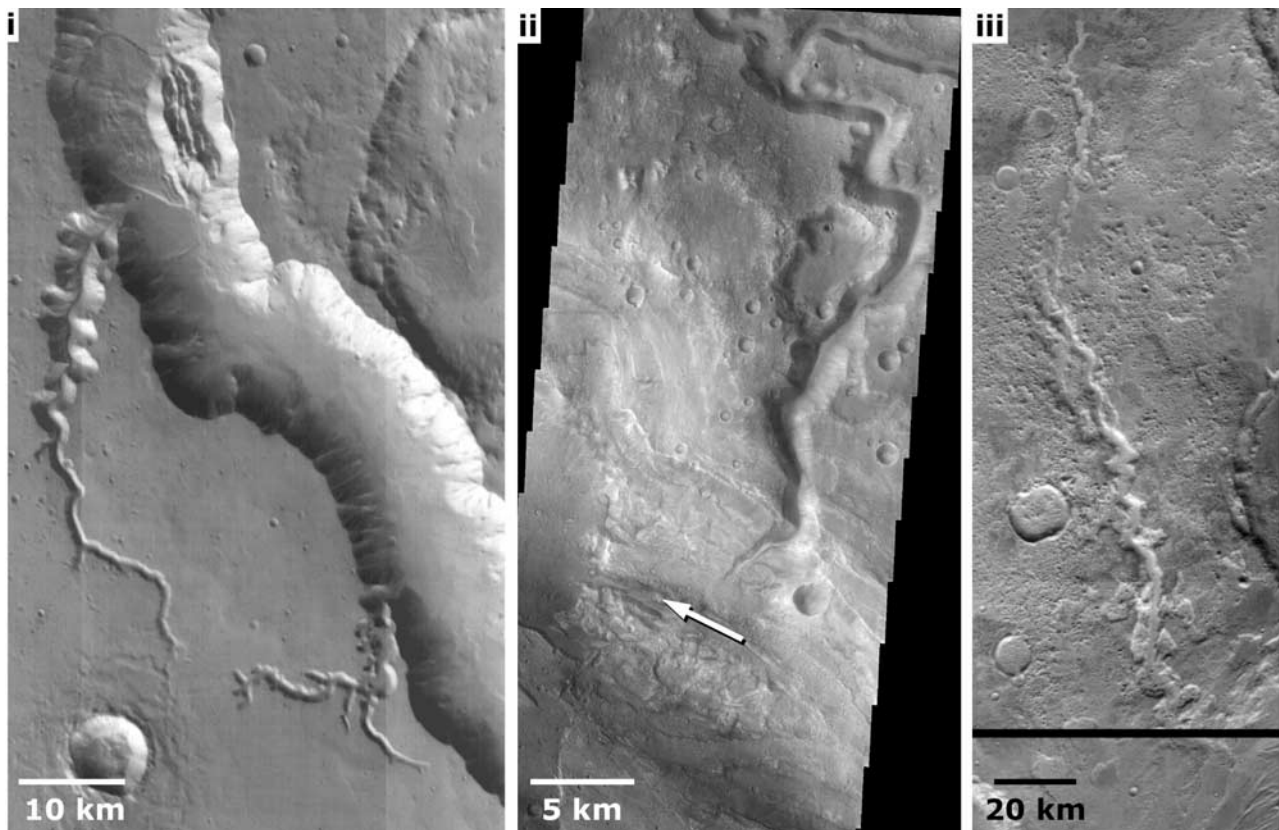


Figure 7a. Sapping morphology associated with outflow channels. (i) THEMIS IR daytime mosaic of sapping tributaries along Shalbatana Vallis. The southern tributary is hanging (confirmed by MOC imagery). (ii) THEMIS visual image of an Ares Vallis tributary (Ares Vallis crosses lower half of image from right to left). Incision of the tributary into the Ares Vallis wall suggests activity no older than late stage flooding in Ares Vallis. (iii) THEMIS IR daytime mosaic of another Ares Vallis tributary. This valley erodes the Ares Vallis walls and floor. (Black strip indicates region of no data.)

[30] The outflow channels are much larger than valley networks, and craters on their floors are numerous enough to provide reasonably reliable age estimates. Together with upper bounds provided by ages of surrounding units, most analyses suggest a Hesperian to early Amazonian age for circum-Chryse outflow channel formation [Tanaka, 1986, and references therein]. Many of these channels have tributaries exhibiting typical sapping morphologies (Figure 7a). Some tributaries appear to have been active as long as their parent outflow channels, while others are hanging, suggesting an earlier cessation of activity. We do not observe dense, dendritic tributary networks along outflow channels.

[31] Sapping networks are also observed on the floors of outflow channels, particularly in Kasei Valles. The largest of these is the Nilus Mensae network which is thought to have postdated fluvial activity in north Kasei Valles, but predated the cessation of activity in south Kasei Valles [Williams *et al.*, 2000] (Figure 7b) constraining its age to the Hesperian.

[32] Sapping morphology is found in the Valles Marineris canyon walls (Figure 8). The Valles Marineris formed between the early Hesperian and Amazonian [Lucchitta *et al.*, 1992] with most recent activity in the west most region of Noctis Labrynthus [Masson, 1980]. One of the most

extensive apparent manifestations of groundwater sapping in the Valles Marineris is Louros Valles [Sharp, 1973; Kochel and Piper, 1986], a system of tributary canyons on the south wall of Ius Chasma (Figure 8a). These tributaries incise late Hesperian basalt flows from Syria Planum volcanic sources (unit Hsu) [Witbeck *et al.*, 1991]. Other examples of tributary canyons include those in Echus Chasma, but due to the complex nature of their superposition with other drainage networks, these features are discussed in detail in the next section.

4.6. Sapping Morphology Associated With Dense Valley Networks

4.6.1. Echus Chasma

[33] Echus Chasma has a group of tributary canyons along its southern and eastern edges (Figure 9) that incise early Hesperian fractured volcanics (unit Hf) [Rotto and Tanaka, 1995] and younger Hesperian volcanic flows (Hsu) [Rotto and Tanaka, 1995]. Also dissecting these units is a recently discovered suite of shallow dense valley networks interpreted by Mangold *et al.* [2004] to have been incised by surface runoff.

[34] The morphologies and spatial relationships of the tributary canyons and dense valley networks provide clues concerning their relative formation times. First, the tributary

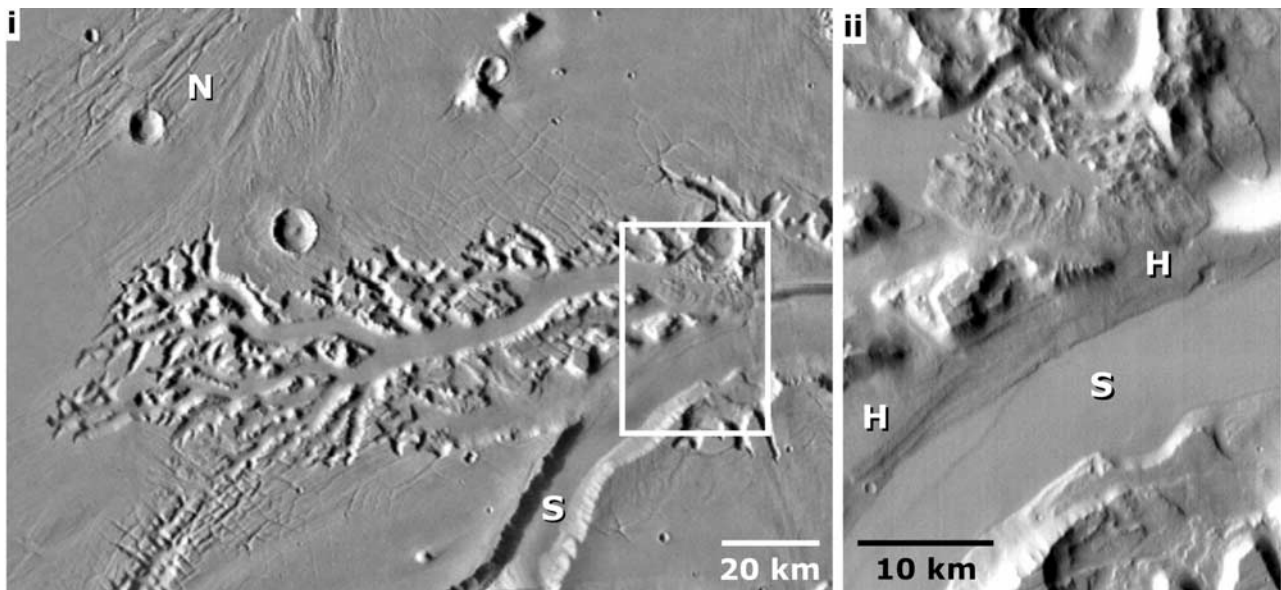


Figure 7b. (i) Viking mosaic of Nilus Mensae, a network of depressions in the Kasei Valles floor interpreted by *Williams et al.* [2000] to be formed by groundwater sapping. The network has theater-like headward termini, apparent structural control (as suggested by the network of fractures to the north), and short tributaries. *Williams et al.* [2000] inferred a period of formation postdating activity in north Kasei Valles (N) but predating the cessation of activity in south Kasei Valles (S). The former time constraint is evident in the western tributaries which incise north Kasei Valles, while the latter constraint is observed in the hanging mouth of the Nilus Mensae network shown in panel ii, a THEMIS IR daytime enlargement of the white box in panel i.

canyons do not appear to have been eroded by fluvial activity in the dense valley networks: their margins are not notched where valley networks intersect them. In fact, several tributary canyons cross-cut individual dense valley network segments (Figure 10). Additionally, the tributary canyon walls and floors do not carry deposits obviously related to dense valley network activity. These observations suggest that tributary canyons postdate dense valley network formation in the region.

[35] The headward termini of some tributary canyons in west Echus Chasma do, however, coincide to some degree with the main branches of certain dense valley networks (Figure 11a). This led *Mangold et al.* [2004] to conclude that dense network and tributary canyon formation were coeval. However, the lack of related erosional or depositional forms in the canyons does not support this view. On the contrary, incision of the valley networks, although apparently shallow in the Echus Chasma region, may have locally lowered the terrain enough to influence the subsequent headward migration of the tributary canyons. (Similar relationships are observed west of Ganges Chasma and along Mamers Vallis; Figures 8d and 13. We note, however, that mass wasting and other non-fluvial processes may have influenced the superposition relations of observed valley morphologies, making their relative timing more difficult to assess.)

[36] Valleys are also observed in narrow (~10 km) bands along the downstream margins of some Echus Chasma tributary canyons (Figure 11b). Analysis of the contact with canyon margins in THEMIS visual images (which have a spatial resolution several times that of THEMIS IR images)

indicate the same relationship described above, namely that canyon rims do not exhibit signs of erosion resulting from fluvial activity in the valleys. Moreover, it is not clear that surface runoff significantly influenced valley formation in these bands, since they do not exhibit the well-developed dendritic form of the larger southwest Echus Chasma networks. Regardless of the relative timing of the two fluvial morphologies, it appears they both must have formed during the Hesperian. The implications of this observation for our central hypothesis are discussed later.

4.6.2. Valley Networks with Pristine and Degraded Morphologies

[37] *Baker and Partridge* [1986] used Viking images to analyze several dense valley networks in the heavily cratered southern highlands. They noted the presence within individual networks of both pristine and degraded valley segments which, they suggested, correlated with groundwater sapping and surface runoff origins, respectively. They used the predominantly downstream placement of pristine segments to conclude that initial valley network formation was influenced by surface runoff, producing the now degraded valleys, while a more recent epoch of groundwater sapping formed the pristine valleys. We noted above that their view has been met with mixed support in more recent analyses. In addition, some intersections of pristine and degraded segments may be explained by a change in lithology along the valley, rather than by distinct episodes or styles of fluvial activity. In particular, *Irwin and Howard* [2002] interpret some pristine and degraded valley intersections as nick points, with downstream (pristine) reaches having eroded through a resistant surface layer, and upstream (degraded)

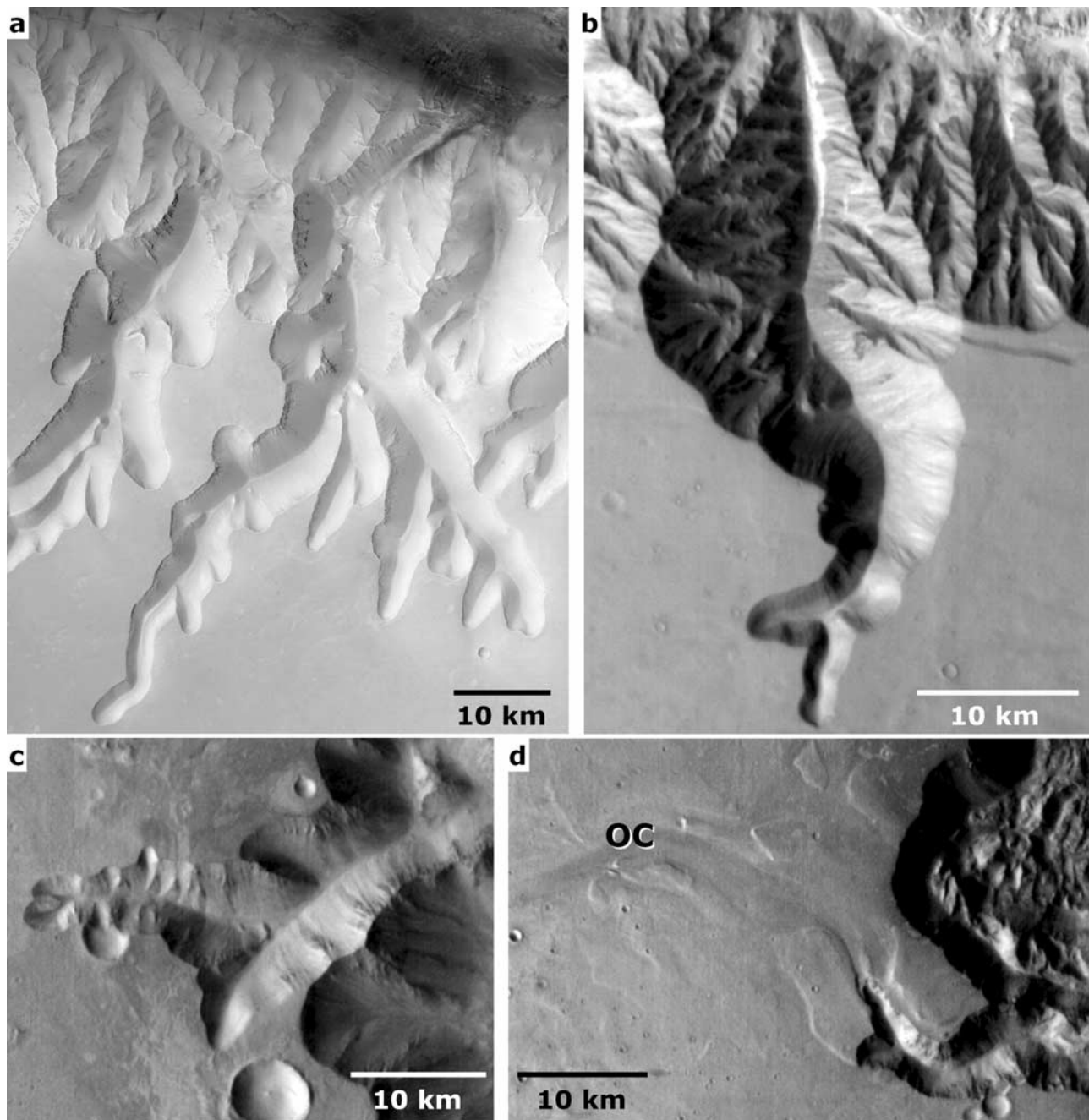


Figure 8. Sapping morphology associated with the Valles Marineris. (a) Mars Express (ESA) HRSC image of Louros Valles in south Ius Chasma. Similar morphologies are observed in THEMIS IR daytime images of (b) south Hebes Chasma and (c) west Ganges Chasma. (d) Another tributary canyon in west Ganges Chasma has captured an outflow channel (OC) originating from an elongate closed depression about 200 km to the west (not shown). THEMIS IR daytime mosaic.

reaches remaining superficially incised. Terrestrial features such as the sapping valleys on the island of Hawaii [Kochel and Piper, 1986] suggest that surface runoff and groundwater sapping can proceed simultaneously, with waterfalls occurring at theater-like headcuts along the valley.

[38] Our own analysis (with THEMIS imagery) of the valley networks mapped by Baker and Partridge [1986] suggests that pristine segments do not consistently occur downstream from degraded segments, a finding that may complicate the simple interpretation of two distinct episodes

of erosion. Additionally, most of the pristine segments identified by Baker and Partridge [1986] are somewhat degraded relative to the large sparse valley networks. Only one valley (Scamander Vallis) mapped by Baker and Partridge [1986] is as pristine as Nanedi Valles, Nirgal Valles, and others, and is the only Baker and Partridge [1986] valley included in our set of sparse networks. This valley also has very few tributaries, most of which seem to be groundwater sapping valleys. Our overall conclusion is that while the Baker and Partridge [1986] valley networks

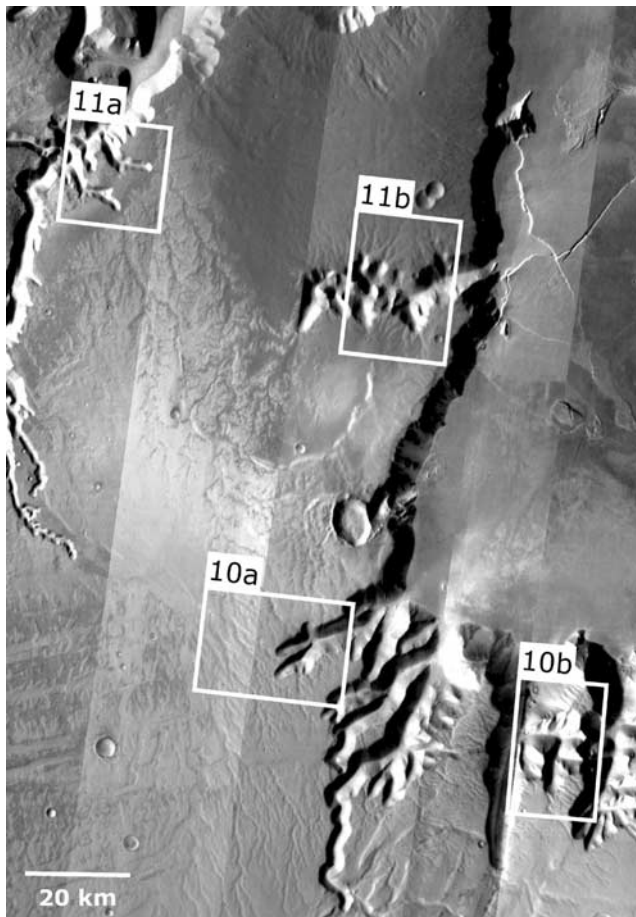


Figure 9. THEMIS IR daytime mosaic of southwest Echus Chasma and adjacent plains. A shallow, densely dissecting valley network system reaches from the bottom center left of the image northward to the large western tributary canyon (top left corner). Smaller networks appear near southern and western canyon margins. White boxes indicate detailed coverage in other figures, as labeled.

may still indicate a regional evolution in fluvial erosive style, other valley systems such as the large sparse networks may provide more conclusive evidence, hence the focus of this paper.

[39] Another example of multiple valley morphologies within a single network is Ma'adim Vallis. The main trunk of the Ma'adim network is terraced, suggesting discrete fluvial episodes, including flooding, response to base level changes, and groundwater sapping [Cabrol *et al.*, 1998a]. Valley floor crater counts suggest fluvial activity spanning the late Noachian to the late Hesperian [Cabrol *et al.*, 1998b]. Cabrol *et al.* [1998a] state that “nowhere on the valley can the hydrographic pattern be compared to a network formed by drainage caused by rainfall.” This picture of a late Noachian to Hesperian episode of erosion negligibly influenced by surface runoff is consistent with our hypothesis. We note, however, that other workers differ on the overall longevity and mode of formation of Ma'adim Valles. Irwin *et al.* [2004] suggest a short-lived episode of flooding at the Noachian-Hesperian boundary, caused by overflow in uplands basins. This implies that surface liquid

water was (episodically) stable and present in large, possibly ice-covered paleolakes at the Noachian-Hesperian boundary, again consistent with our hypothesis, but not conclusive.

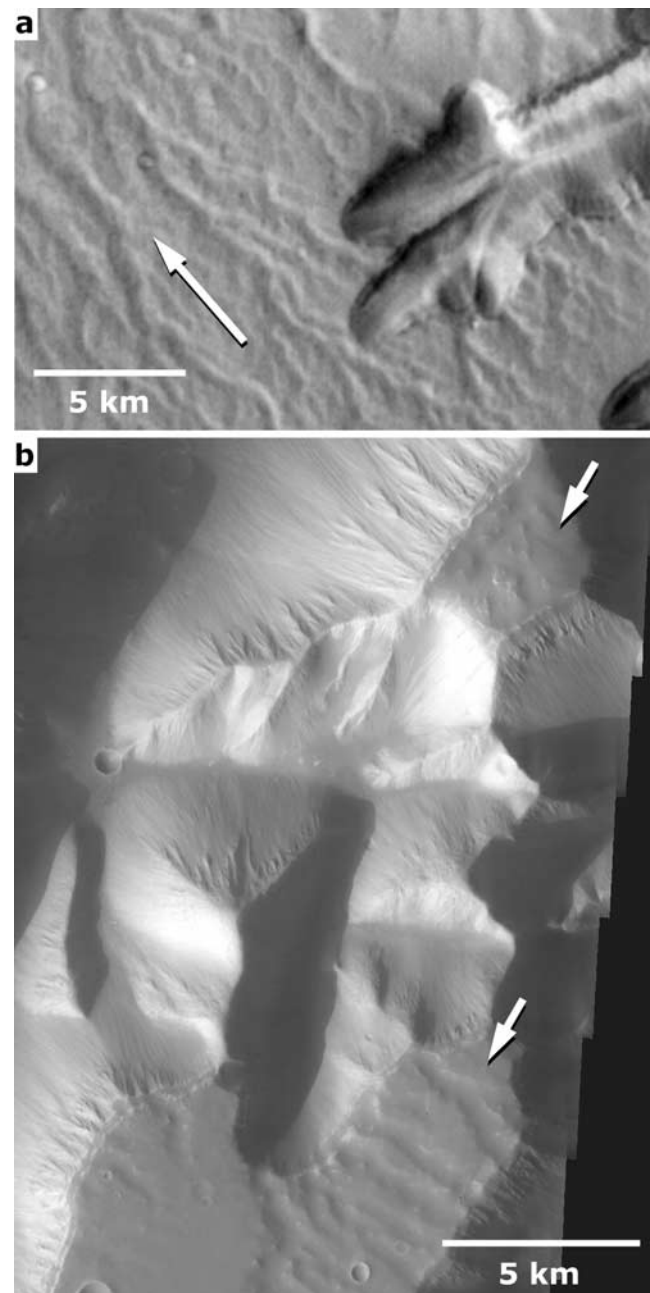


Figure 10. (a) A tributary canyon likely formed by groundwater sapping incises plains covered with densely dissecting fluvial valleys west of Echus Chasma (see Figure 9). The canyon is at right angles to the flow direction of the valley network (arrow) and does not appear to have influenced valley placement [see Mangold *et al.*, 2004, Figure 2]. THEMIS IR daytime. (b) South of Echus Chasma, sections of plateau incised by valley networks appear to have been isolated into mesas (arrows) by subsequent groundwater sapping and aeolian processes. The floor of Echus Chasma is visible at the top of the image. THEMIS visual.

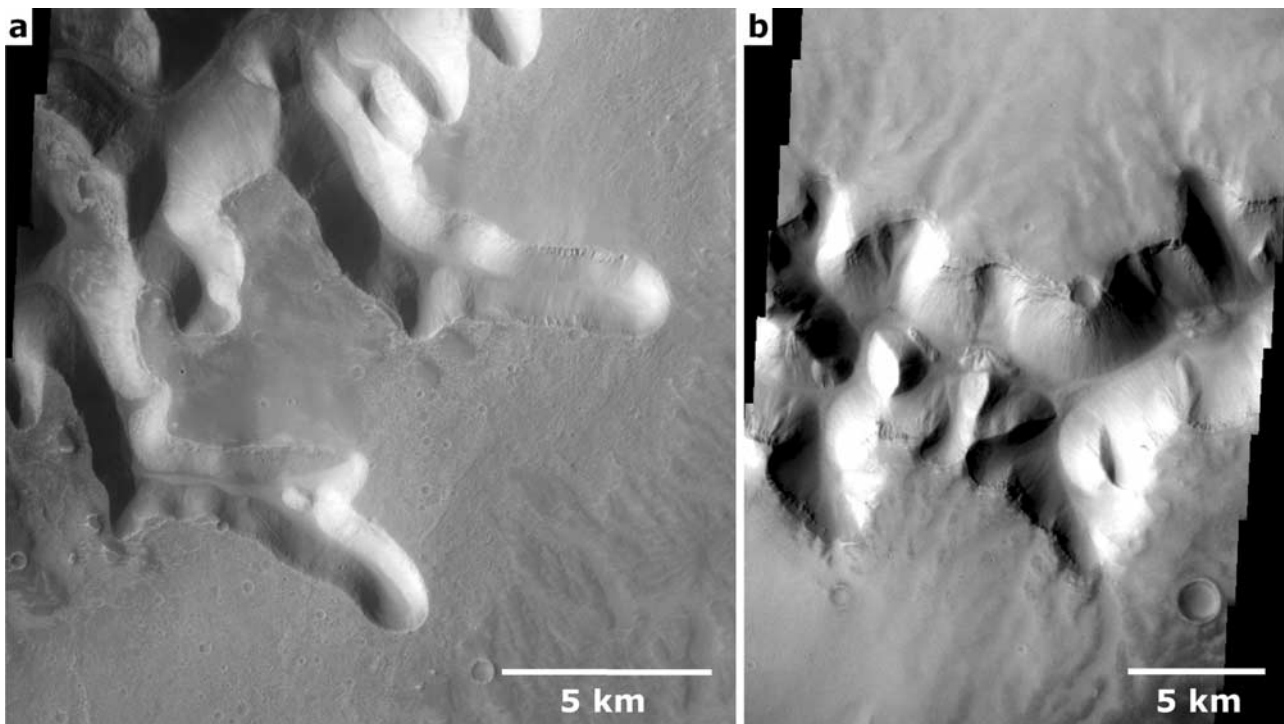


Figure 11. (a) Two canyon tributaries west of Echus Chasma are each seen in lower-resolution images (e.g., Figure 9) to coincide with a shallow, high-order valley network trunk on the adjacent plains. The high-resolution THEMIS visual image here shows that the unit incised by the shallow valley networks (darker ridged unit to right) does not reach the tributary canyon heads and that the canyon margins are pristine. (b) Short, poorly developed valleys intersect with a canyon tributary west of Echus Chasma. It is not clear what process formed these valleys (it may have been groundwater sapping), and while they coincide with canyon head regions, the canyon margins do not appear to be eroded by individual valleys. THEMIS visual image.

[40] Other examples of spatially correlated valley network morphologies include two tributary systems of Mamers Vallis (Figures 12 and 13). In both examples, groundwater sapping appears to have been the most recent fluvial process. As with the highlands networks though, it is difficult to constrain the absolute age of each fluvial epoch.

5. Concluding Discussion

[41] The preceding analyses point toward a late Noachian to early Hesperian formation for large groundwater sapping valley networks on Mars. In addition, those valley networks associated with, and no older than, Hesperian chasmata and outflow channels, appear to be groundwater-controlled, suggesting contemporary climatic conditions unsuitable for surface runoff. These observations, together with the Noachian age of most dense valley networks, support our central hypothesis that surface runoff declined during the late Noachian, leaving erosion by groundwater processes as the predominant means of valley network formation.

[42] Despite their general consensus, the preceding analyses do suggest specific deviations. The increasing distance to Tharsis with age in sparse valley networks (discussed above), together with the Hesperian age of the Echus Chasma dense valley networks (and, perhaps, Melas Chasma networks [Mangold *et al.*, 2004]), suggest that

our hypothesized decrease in surface runoff in favor of groundwater control may have occurred on Tharsis after its cessation elsewhere on the planet. Harrison and Grimm [2004] note that Hesperian volcanic activity at Tharsis was likely characterized by heat fluxes elevated relative to the declining global average, resulting in a regionally thinned (and perhaps locally obliterated) cryosphere, allowing basal melting to occur under thinner ice sheets and perhaps permitting localized direct infiltration of precipitation (delivered at greater rates during periods of high planetary obliquity [Jakosky and Carr, 1985]). In addition, the release of volatiles from Tharsis volcanism [Phillips *et al.*, 2001] and from circum-Chryse outflow channel flooding may temporarily have boosted the regional atmospheric volatile budget, resulting in greater precipitation rates. We note that the possibly delayed fluvial transition at Tharsis may make the Figure 2 transition appear more gradual than it actually was. Put differently, global climate change, the driving process behind our hypothesized transition, may have occurred on a shorter timescale than suggested by the fluvial transition of Figure 2. Regional fluvial erosion would have responded on a similarly short timescale, with the exception of a delay at Tharsis due to its prolonged influence on precipitation and infiltration.

[43] A key observation of the preceding analyses is the small number and large size of groundwater-controlled valleys. This may be related to characteristics of the

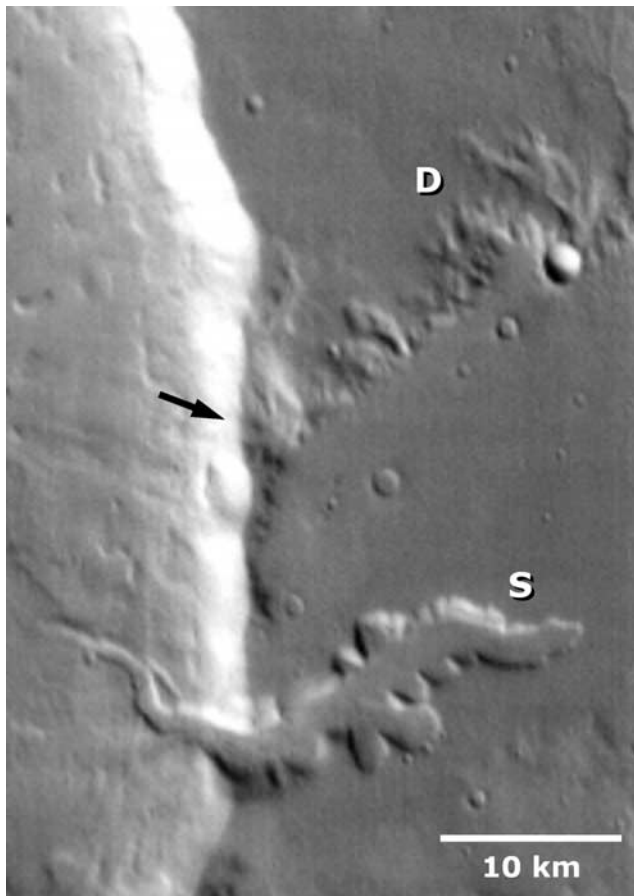


Figure 12. An example of local evolution in fluvial processes. The floor of Mamers Vallis occupies the left side of the image. It cuts through an impact crater with densely dissecting valley networks on its northern rim (D). A sapping valley (S) connects the crater floor with Mamers Vallis. Mamers Vallis appears to cut across the densely dissecting valley networks (arrow) but is itself incised by the sapping valley; hence the sapping valley must be younger than the dense valley networks. The valley networks likely delivered water to an aquifer in the crater floor, which was later drained by sapping. THEMIS IR daytime image.

contemporary water table. In previous epochs (early to middle Noachian) precipitation rates were likely relatively high (although perhaps episodically so), forcing the water table to form a subdued replica of the surface topography [Tóth, 1963]. Discharge would have occurred in the many local topographic lows where water table and surface intersected. Each source of discharge would be able to draw from only a limited reservoir of groundwater due to competition with neighboring sources. The subsequent (late Noachian) decrease in atmospheric water vapor content due to climate change would have started to decouple precipitation from the aquifer [Clifford and Parker, 2001], allowing the water table to shed its smaller wavelengths and replicate only the larger topographic features. This would have reduced the number of discharge zones to the fewer topographic minima of a similar scale, while increasing the aquifer volume supplying each zone. This may have

resulted in the formation of large sapping networks. Indeed, the generally high elevation of southern highlands valley networks [Carr and Clow, 1981] and the relatively lower elevation of large sparse networks [Carr, 2002], while not conclusively supported by our rudimentary global statistical analysis, may nonetheless hint at such an evolution in water table elevation, and may coincide with the elevation changes envisioned for the northern plains by Tanaka *et al.* [2003]. We do note, however, that a simple model of headward erosion by groundwater sapping at discharge locations may not adequately explain some features of groundwater-controlled valleys, such as meanders, and may have to include upstream sources of groundwater [Carr and Malin, 2000].

[44] Next, we highlight the role of pore ice in groundwater-controlled fluvial erosion. Large sapping valleys such as Nandedi and Nirgal Valles may have been influenced by a thin incipient cryosphere. However, the somewhat younger and shallower sapping features at Hesperian chasmata and outflow channels likely formed when a relatively thick cryosphere was already in place. Estimated Hesperian surface temperatures [e.g., Clifford, 1993] and recent geothermal heat flux estimates ($\sim 30 \text{ mW/m}^2$ [McGovern *et al.*, 2002]) yield a low latitude cryosphere a few kilometers thick, somewhat greater than the 1 to 2 km relief of chaotic terrains [Carr, 1979] and significantly greater than the headward depths of outflow channel sapping tributaries. A groundwater source at shallow depths must therefore be provided by basal melting of thick ice sheets [Carr and Head, 2003], cryosphere melting by volcanic heat, or episodic periods of warmer climate permitting groundwater flow (sourced by melting or precipitation) in a shallow

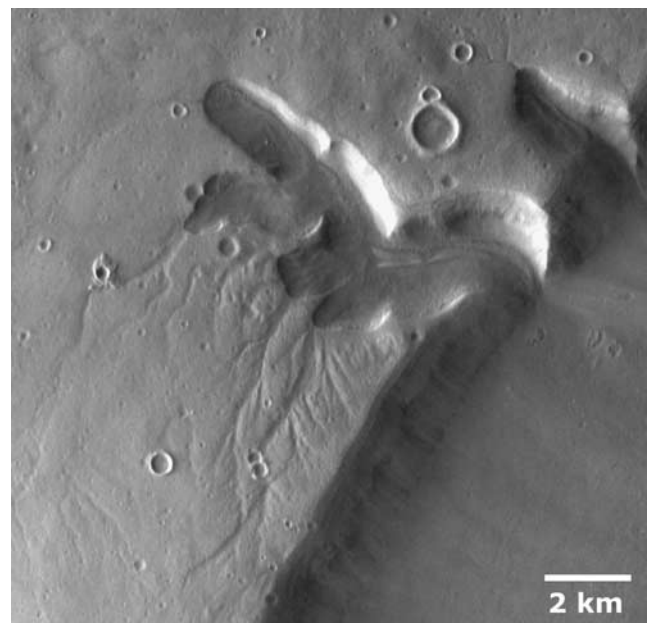


Figure 13. A sapping tributary of Mamers Vallis incises a shallow, densely dissecting valley network system. The headward margins of the sapping tributary do not show signs of erosion by fluvial activity in the smaller valleys, suggesting that surface runoff influenced only the earliest stage of dissection in this region. THEMIS visual image.

Table A1. Location and Identity of Images Appearing in the Figures^a

Figure	Lat.	Lon.	Image Number
1a	42°S	267°E	I05459002, I01714004, I02800002, I01689003, I05409002
1b	3°N	311°E	I08590012, I01150003, I01849010
3a	8.5°N	312°E	V01849011
3b	11.5°	313°E	I01125002
4	21°N	303°E	I02536005, I10662011, I0251105, I08091021, I10013010, I09389011, I02461007, I08041038
5	27.5°S	315.5°E	I07617002, I07979003, I01650002, I02736002, I03460002, I01625004, I02711004, I01962002
6a	31°N	20°E	I05030007
6b	33°N	18°E	V05829012
6c	36°N	26.5°E	I02633002, I11670004, I04493005
6d	37°N	35°E	I01684006
(7a i)	4°N	316°E	I07691024, I08053025, I08777013
(7a ii)	6.5°N	341°E	V08152028
(7a iii)	8.5°N	339°E	I02647002, I01898005, I02622005, I011659008, I11347010, I02597002
(7b i)	22°N	287.5°E	Viking MDIM 2 mosaic generated by U.S. Geol. Surv. online PDS MAP-A-PLANET facility
(7b ii)	22°N	289°E	I03223002
8a	9°	279°E	Mars Express HRSC image (ESA)
8b	2°S	284.5°E	I01076010
8c	8°S	307°E	I06394003, I09526014
8d	8.5°S	307°E	I07504023, I09526014
9	0°N	279°E	I00839002, I01251014, I01875013, I01925006, I01950002, I02649009, I02986002, I06419047, I06444027, I06706023, I06731015, I06781017, I06831005, I07068015, I07093014, I07143016, I07193011, I07455014, I07480016, I07505017, I07867021
10a	1°S	279°E	I06781017
10b	1°S	279.5°E	V08230001
11a	0.5°N	278°E	V10176016
11b	0°N	279°E	V01925007
12	33°N	18°E	I01385006
13	37°N	15°E	V06291019

^aNumbers preceded by “I” and “V” denote THEMIS infrared and visual images, respectively.

subsurface layer. If this last case is important, the episodes of warm climate would, according to our hypothesis, likely have produced little surface runoff, a view supported by the predominance (and younger age) of groundwater sapping tributaries.

[45] To conclude, we describe a possible terrestrial analog for our fluvial evolution hypothesis. *Hoke et al.* [2004] attribute a groundwater sapping origin to large fluvial canyons (quebradas) crosscutting parallel valley networks in the Western Cordillera Mountains of the Chilean Atacama Desert. They claim that a decrease in precipitation in the region several Myr ago led to a transition from surface runoff (which carved the dense, parallel networks) to groundwater sapping (which carved the canyons). Age dating and isotopic analysis of water from seepage faces in the canyon headwalls suggest a several thousand year transit of groundwater from high elevation recharge zones in the east. The morphology of the canyons has much in common with that of Martian sparse networks, including widths of several km, theater-like head regions, and few tributaries.

Appendix A: Identification of Images

[46] We present in Table A1 the approximate central spatial coordinates of figures used in this work and the identities of contributing images. We use mostly THEMIS daytime IR images (eight digits prefaced by the letter “I”) or visual images (prefaced by “V”). Other instruments are named explicitly in Table A1.

[47] **Acknowledgments.** This work was supported by internal research funds from Southwest Research Institute project R9428. We thank

Alan Howard, Roger Phillips, and Mark Bullock for their insightful reviews.

References

- Baker, V. R. (1982), *The Valleys of Mars*, Univ. of Tex. Press, Austin.
- Baker, V. R., and J. B. Partridge (1986), Small Martian valleys: Pristine and degraded morphology, *J. Geophys. Res.*, *91*, 3561–3572.
- Bibring, J.-P., et al. (2005), Mars surface diversity as revealed by the OMEGA/Mars Express observations, *Science*, *307*, 1576–1581.
- Cabrol, N. A., and E. A. Grin (2001), Composition of the drainage network on early Mars, *Geomorphology*, *37*, 269–287.
- Cabrol, N. A., E. A. Grin, and R. Landheim (1998a), Ma’adim Valles evolution: Geometry and models of discharge rate, *Icarus*, *132*, 362–377.
- Cabrol, N. A., E. A. Grin, R. Landheim, R. O. Kuzmin, and R. Greeley (1998b), Duration of the Ma’adim Vallis/Gusev Crater Hydrogeologic System, Mars, *Icarus*, *133*, 98–108.
- Carr, M. H. (1979), Formation of Martian flood features by release of water from confined aquifers, *J. Geophys. Res.*, *84*, 2995–3007.
- Carr, M. H. (1996), *Water on Mars*, Oxford Univ. Press, New York.
- Carr, M. H. (2001), Mars Global Surveyor observations of Martian fretted terrain, *J. Geophys. Res.*, *106*, 23,571–23,594.
- Carr, M. H. (2002), Elevations of water-worn features on Mars: Implications for circulation of groundwater, *J. Geophys. Res.*, *107*(E12), 5131, doi:10.1029/2002JE001845.
- Carr, M. H., and F. C. Chuang (1997), Martian drainage densities, *J. Geophys. Res.*, *102*(E4), 9145–9152.
- Carr, M. H., and G. D. Clow (1981), Martian valleys and valleys: Their characteristics, distribution, and age, *Icarus*, *48*, 91–117.
- Carr, M. H., and J. W. Head III (2003), Basal melting of snow on early Mars: A possible origin of some valley networks, *Geophys. Res. Lett.*, *30*(24), 2245, doi:10.1029/2003GL018575.
- Carr, M. H., and M. C. Malin (2000), Meter-scale characteristics of Martian valleys and valleys, *Icarus*, *146*, 366–386.
- Carruthers, M. W., and G. E. McGill (1998), Evidence for igneous activity and implications for the origin of a fretted valley in southern Ismenius Lacus, Mars, *J. Geophys. Res.*, *103*(E13), 31,433–31,443.
- Chapman, C. R., and K. L. Jones (1977), Cratering and obliteration history of Mars, *Annu. Rev. Earth Planet Sci.*, *5*, 515–540.
- Christensen, P. R., and S. W. Ruff (2004), Formation of the hematite-bearing unit in Meridiani Planum: Evidence for deposition in standing water, *J. Geophys. Res.*, *109*, E08003, doi:10.1029/2003JE002233.

- Clifford, S. M. (1993), A model for the hydrologic and climatic behavior of water on Mars, *J. Geophys. Res.*, *98*, 10,973–11,016.
- Clifford, S. M., and T. J. Parker (2001), The evolution of the Martian hydrosphere: Implications for the fate of a primordial ocean and the current state of the northern plains, *Icarus*, *154*, 40–79.
- Craddock, R. A., and A. D. Howard (2002), The case for rainfall on a warm, wet early Mars, *J. Geophys. Res.*, *107*(E11), 5111, doi:10.1029/2001JE001505.
- Dohm, J. M., R. C. Anderson, V. R. Baker, R. G. Strom, G. Komatsu, and T. M. Hare (2000), Pulses of magmatic activity through time: Potential triggers for climatic variations on Mars, *Proc. Lunar Planet. Sci. Conf. 31st*, Abstract 1632.
- Fetter, C. W. (1994), *Applied Hydrogeology*, 3rd ed., Prentice-Hall, Upper Saddle River, N. J.
- Golombek, M. P., J. A. Grant, L. S. Crumpler, R. Greeley, and R. E. Arvidson (2005), Climate change from the Mars Exploration Rover landing sites: From wet in the Noachian to dry and desiccating since the Hesperian, *Proc. Lunar Planet. Sci. Conf. 36th*, Abstract 1539.
- Grant, J. A., and T. J. Parker (2002), Drainage evolution in the Margaritifer Sinus region, Mars, *J. Geophys. Res.*, *107*(E9), 5066, doi:10.1029/2001JE001678.
- Grant, J. A., and P. H. Schultz (1993), Degradation of selected terrestrial and Martian impact craters, *J. Geophys. Res.*, *98*(E6), 11,025–11,042.
- Greeley, R., J. E. Guest, D. H. Scott, and K. L. Tanaka (1987), Geologic map of the Eastern, Western, and Polar regions of Mars, *U.S. Geol. Surv. Misc. Invest. Ser.*, *I-1802a*, *I-1802b*, and *I-1802c*.
- Haberle, R. M. (1998), Early Mars climate models, *J. Geophys. Res.*, *103*, 28,467–28,480.
- Harrison, K. P., and R. E. Grimm (2004), Tharsis recharge: A source of groundwater for Martian outflow channels, *Geophys. Res. Lett.*, *31*, L14703, doi:10.1029/2004GL020502.
- Hartmann, W. K., and G. Neukum (2001), Cratering chronology and the evolution of Mars, *Space Sci. Rev.*, *96*, 165–194.
- Hartmann, W. K., G. Ryder, L. Dones, and D. Grinspoon (2000), The time-dependent intense bombardment of the primordial Earth/Moon system, in *Origin of the Earth and Moon*, edited by R. M. Canup and K. Righter, pp. 493–512, Univ. of Ariz. Press, Tucson.
- Hoke, G. D., B. L. Isacks, T. E. Jordan, and J. S. Yu (2004), Groundwater-sapping for the giant quebradas of northern Chile, *Geology*, *32*, 605–608.
- Hynek, B. M., and R. J. Phillips (2001), Evidence for extensive denudation of the Martian highlands, *Geology*, *29*, 407–410.
- Irwin, R. P., III, and A. D. Howard (2002), Drainage basin evolution in Noachian Terra Cimmeria, Mars, *J. Geophys. Res.*, *107*(E7), 5056, doi:10.1029/2001JE001818.
- Irwin, R. P., III, A. D. Howard, and T. A. Maxwell (2004), Geomorphology of Ma'adim Vallis, Mars, and associated paleolake basins, *J. Geophys. Res.*, *109*, E12009, doi:10.1029/2004JE002287.
- Irwin, R. P., T. A. Maxwell, A. D. Howard, R. A. Craddock, and J. M. Moore (2005), A Noachian/Hesperian hiatus and erosive reactivation of Martian valley networks, *Proc. Lunar Planet. Sci. Conf. 36th*, Abstract 2221.
- Jakosky, B. M., and M. H. Carr (1985), Possible precipitation of ice at low latitudes of Mars during periods of high obliquity, *Nature*, *315*, 559–561.
- Jakosky, B. M., and L. Leshin (2001), Mars D/H: Implications for volatile evolution and climate history, *AGU Spring*, Abstract #P32A-04.
- Jakosky, B. M., and R. J. Phillips (2001), Mars' volatile and climate history, *Nature*, *412*, 237–244.
- Jaumann, R., and D. Reiss (2002), Nirgal Vallis: Evidence for extensive sapping, *Proc. Lunar Planet. Sci. Conf. 33rd*, Abstract 1579.
- Kasting, J. F. (1991), CO₂ condensation and the climate of early Mars, *Icarus*, *94*, 1–13.
- Kochel, R. C., and J. Piper (1986), Morphology of large valleys on Hawaii: Evidence for groundwater sapping and comparisons with Martian valleys, *Proc. Lunar Planet. Sci. Conf. 17th*, Part 1, *J. Geophys. Res.*, *91*, suppl., E175–E192.
- Laity, J. E., and M. C. Malin (1985), Sapping processes and the development of theater-headed valley networks on the Colorado Plateau, *Geol. Soc. Am. Bull.*, *96*, 203–217.
- Laskar, J., A. C. M. Correia, M. Gastineau, F. Joutel, B. Lévraud, and P. Robutel (2004), Long term evolution and chaotic diffusion of the insolation quantities of Mars, *Icarus*, *170*, 343–364.
- Lucchitta, B. K., A. S. McEwen, G. D. Clow, P. E. Geissler, R. B. Singer, R. A. Schultz, and S. W. Squyres (1992), The canyon system on Mars, in *Mars*, edited by H. H. Keffer et al., pp. 453–492, Univ. of Ariz. Press, Tucson.
- Luhmann, J. G., R. E. Johnson, and M. H. G. Zhang (1992), Evolutionary impact of sputtering of the Martian atmosphere by O⁺ pickup ions, *Geophys. Res. Lett.*, *19*, 2151–2154.
- Malin, M. C., and K. S. Edgett (2003), Evidence for persistent flow and aqueous sedimentation on early Mars, *Science*, *302*, 1931–1934.
- Mangold, N., C. Quantin, V. Ansan, C. Delacourt, and P. Allemand (2004), Evidence for precipitation on Mars from dendritic valleys in the Valles Marineris area, *Science*, *305*, 78–81.
- Masson, P. (1980), Contribution to the structural interpretation of the Valles Marineris-Noctis Labyrinthus-Claritas Fossae regions of Mars, *Moon Planets*, *22*, 211–219.
- Masursky, H. (1973), An overview of geologic results from Mariner 9, *J. Geophys. Res.*, *78*, 4037–4047.
- McEwen, A. S. (2003), Secondary cratering on Mars: Implications for age dating and surface properties, in *6th International Conference on Mars*, Abstract 3268, Lunar and Planet. Inst., Houston, Tex.
- McGill, G. E. (2000), Crustal history of north central Arabia Terra, Mars, *J. Geophys. Res.*, *105*(E3), 6945–6959.
- McGovern, P. J., S. C. Solomon, D. E. Smith, M. T. Zuber, M. Simons, M. A. Wicczorek, R. J. Phillips, G. A. Neumann, O. Aharonson, and J. W. Head (2002), Localized gravity/topography admittance and correlation spectra on Mars: Implications for regional and global evolution, *J. Geophys. Res.*, *107*(E12), 5136, doi:10.1029/2002JE001854.
- Melosh, H. J., and A. M. Vickery (1989), Impact erosion of the primordial atmosphere of Mars, *Nature*, *338*, 487–489.
- Mischna, M. A., J. F. Kasting, A. Pavlov, and R. Freedman (2000), Influence of carbon dioxide clouds on early Martian climate, *Icarus*, *145*, 546–554.
- Mischna, M. A., M. I. Richardson, R. J. Wilson, and D. J. McCleese (2003), On the orbital forcing of Martian water and CO₂ cycles: A general circulation model study with simplified volatile schemes, *J. Geophys. Res.*, *108*(E6), 5062, doi:10.1029/2003JE002051.
- Mitchell, D. L., R. P. Lin, C. Mazelle, H. Rème, P. A. Cloutier, J. E. P. Connerney, M. H. Acuña, and N. F. Ness (2001), Probing Mars' crustal magnetic field and ionosphere with the MGS Electron Reflectometer, *J. Geophys. Res.*, *106*, 23,419–23,428.
- Moore, J. M., A. D. Howard, W. E. Dietrich, and P. M. Schenk (2003), Martian Layered Fluvial Deposits: Implications for Noachian Climate Scenarios, *Geophys. Res. Lett.*, *30*(24), 2292, doi:10.1029/2003GL019002.
- Neukum, G., and K. Hiller (1981), Martian ages, *J. Geophys. Res.*, *86*, 3097–3121.
- Owen, T., J. P. Maillard, C. de Bergh, and B. L. Lutz (1988), Deuterium on Mars—The abundance of HDO and the value of D/H, *Science*, *240*, 1767–1770.
- Parker, T. J., R. S. Saunders, and D. M. Schneeburger (1989), Transitional morphology in west Deuteronilus Mensae, Mars: Implications for modification of the lowland/upland boundary, *Icarus*, *82*, 111–145.
- Phillips, R. J., et al. (2001), Ancient geodynamics and global-scale hydrology on Mars, *Science*, *291*, 2587–2591.
- Pieri, D. C. (1976), Martian valleys: Distribution of small valleys on the Martian surface, *Icarus*, *27*, 25–50.
- Pollack, J. B., J. F. Kasting, S. M. Richardson, and K. Poliakov (1987), The case for a wet, warm climate on early Mars, *Icarus*, *71*, 203–224.
- Rotto, S., and K. L. Tanaka (1995), Geologic/geomorphic map of the Chryse Planitia region of Mars, *U.S. Geol. Surv. Misc. Invest. Ser.*, *Map I-2441*.
- Schubert, G., S. C. Solomon, D. L. Turcotte, M. J. Drake, and N. H. Sleep (1992), Origin and thermal evolution of Mars, in *Mars*, edited by H. H. Keffer et al., pp. 147–183, Univ. of Ariz. Press, Tucson.
- Scott, D. H., and J. M. Dohm (1992), Mars highland valleys: An age reassessment, *Proc. Lunar Planet. Sci. Conf. 23rd*, 1251–1252.
- Segura, T. L., O. B. Toon, A. Colaprete, and K. Zahnle (2002), Environmental effects of large impacts on Mars, *Science*, *298*, 1977–1980.
- Sharp, R. P. (1973), Mars: Troughed terrain, *J. Geophys. Res.*, *78*, 4063–4072.
- Sharp, R. P., and M. C. Malin (1975), Valleys on Mars, *Geol. Soc. Am. Bull.*, *86*, 593–609.
- Squyres, S. W., et al. (2004), In situ evidence for an ancient aqueous environment at Meridiani Planum, Mars, *Science*, *306*, 1709–1714.
- Stevenson, D. J. (2001), Mars' core and magnetism, *Nature*, *412*, 214–219.
- Sugiura, N., and H. Hoshino (2000), Hydrogen-isotopic compositions in Allan Hills 84001 and the evolution of the Martian atmosphere, *Meteorit. Planet. Sci.*, *35*, 373–380.
- Tanaka, K. L. (1986), The stratigraphy of Mars, *J. Geophys. Res.*, *91*(B13), E139–E158.
- Tanaka, K. L., J. A. Skinner Jr., T. M. Hare, T. Joyal, and A. Wenker (2003), Resurfacing history of the northern plains of Mars based on geologic mapping of Mars Global Surveyor data, *J. Geophys. Res.*, *108*(E4), 8043, doi:10.1029/2002JE001908.

- Tóth, J. (1963), A theoretical analysis of groundwater flow in small drainage basins, *J. Geophys. Res.*, *68*, 4795–4812.
- Williams, R. M., and R. J. Phillips (2001), Morphometric measurements of Martian valley networks from Mars Orbiter Laser Altimeter (MOLA) data, *J. Geophys. Res.*, *106*, 23,737–23,751.
- Williams, R. M., R. J. Phillips, and M. C. Malin (2000), Flow rates and duration within Kasei Valles, Mars: Implications for the formation of a Martian ocean, *Geophys. Res. Lett.*, *27*, 1073–1076.
- Witbeck, N. E., K. L. Tanaka, and D. H. Scott (1991), Geologic map of the Valles Marineris region, Mars, *U.S. Geol. Surv. Misc. Inv. Ser., Map I-2010*.
-
- R. E. Grimm and K. P. Harrison, Southwest Research Institute, 1050 Walnut Street, Suite 400, Boulder, CO 80302, USA. (grimm@boulder.swri.edu; harrison@boulder.swri.edu)